



## 3D HOMOLOGY MODEL OF THE $\alpha$ 2B-ADRENERGIC RECEPTOR SUBTYPE

Liliana OSTOPOVICI-HALIP,\* Ana BOROTA, Alexandra GRUIA, Maria MRACEC,  
Ramona RAD CURPAN, Mircea MRACEC

Roumanian Academy, Institute of Chemistry Timisoara, 24 M.Viteazul Av., RO-300223, Timișoara, Roumania

Received September 30, 2009

Modeling of human  $\alpha$ 2B-adrenergic receptor subtype ( $\alpha$ 2B-AR) based on the X-ray structure of human  $\beta$ 2-adrenergic receptor (PDB accession code: 2RH1) is reported. The sequence of  $\alpha$ 2B-AR subtype was aligned with the sequence of 2RH1 template and the resulted alignment was used as input for the homology modeling step. The stereochemical quality of the homology model was computed with Procheck software and was found to be in normal ranges. Additionally, the model was confirmed by docking the endogen ligand of all adrenergic receptors (norepinephrine) the results being compared with the ones obtained from mutagenesis-studies. The final model supports the experimental data obtained through site-directed mutagenesis and provides evidence that it can be used in further studies.

### INTRODUCTION

The  $\alpha$ 2B-adrenergic receptor ( $\alpha$ 2B-AR) belongs to the  $\alpha$ 2 class of adrenoceptors, which are members of the G protein coupled receptor (GPCR) family 1. It is distributed mainly in peripheral tissues<sup>1,2</sup> and was cloned and characterized by Lefkowitz<sup>3</sup> and Hartig.<sup>4</sup> Alpha2B-AR mediates important physiological responses, such as salt-induced hypertension,<sup>5</sup> vasoconstrictor response to  $\alpha$ 2-AR agonist<sup>6,7</sup> gastric mucosal defense,<sup>8</sup> antinoceptive effect of N<sub>2</sub>O and possible other antinoceptive responses in the spinal cord,<sup>9,10</sup> increase in the contractions in the pregnant myometrium,<sup>11</sup> and it has an important role in developmental and reproductive processes.<sup>12,13</sup> In 2001 Liggett et al<sup>14</sup> showed that a polymorphic deletion of three intracellular acidic residues (Glu301-Glu302-Glu303) of the  $\alpha$ 2B-adrenergic receptor decreased G protein-coupled receptor kinase-mediated phosphorylation and desensitization. Other important polymorphisms in the promoter region of human  $\alpha$ 2B-AR gene were identified in 2004.<sup>15</sup> No significant difference has

been discovered between the three genotypes of insertion/deletion (I/D) polymorphism of ADRA2B gene and the clinical characteristics of the subjects presenting essential hypertension,<sup>16</sup> however, an I/D polymorphism in the  $\alpha$ 2B adrenoceptor gene was associated with peripheral neuropathy in patients with type 2 diabetes mellitus.<sup>17</sup> The frequency of D allele (of  $\alpha$ 2B-AR gene located on chromosome 2) in type 2 diabetic patients is higher than that of controls and ascertains an increased risk for earlier onset of diabetes.<sup>18</sup> Experimental data have shown that a deletion variant of the  $\alpha$ 2B-AR is related to emotional memory,<sup>19</sup> while the  $\alpha$ 2B-AR polymorphism combined with job strain and decision latitude is associated with higher blood pressures in men.<sup>20</sup> All these physiological responses are due both to the distribution of  $\alpha$ 2B-AR in various tissues and its structure. Similarly to all GPCR, the  $\alpha$ 2B-AR has seven helical transmembranar regions connected by six loops (three intracellular (IL) and three extracellular (EL)). The helical bundle of the seven

\* Corresponding author: [lili.ostopovici@gmail.com](mailto:lili.ostopovici@gmail.com)

transmembranes embeds the binding cavity which is placed at about 10-15 Å distance from the extracellular part of the receptor. The agonists like norepinephrine, interact with key amino acids in the binding domain and induce the coupling to the Gi protein, triggering a chain of events which lead to above mentioned physiological responses. The work presented in this paper is part of a laborious project in progress in our group and dedicated to the discovery of selective antagonists for the  $\alpha$ 2-adenoreceptor family. Here in, we are reporting the building and refining of a 3D homology model for  $\alpha$ 2B-AR based on the recently published X-ray structure of human  $\beta$ 2-AR.<sup>21</sup> Until now, several homology models<sup>22,23</sup> for  $\alpha$ 2B-AR have been reported, but all of them were built based on the X-ray structure of rhodopsin. As the X-ray structure of the human  $\beta$ 2-adrenergic receptor (h $\beta$ 2-AR) has been solved recently,<sup>21</sup> we think that for functional reasons a more appropriate model should be obtained using the 2RH1 structure as template in the homology modeling process. Like  $\alpha$ 2-ARs, the  $\beta$ 2-AR belongs to the same subfamily of GPCR and binds endogenously the same biogenic amine, norepinephrine (nor-adrenaline).

## METHODS

The sequence of the h $\alpha$ 2B-AR was taken from SwissProt database<sup>24</sup> and it was aligned with the sequence of the template structure downloaded from Protein Data Bank. The sequence alignment was automatically generated with T-coffee<sup>25, 26</sup> server and manually refined according to the template structure. The homology modeling package Modeller<sup>27</sup> (version 9v6) was used to obtain the three-dimensional model for  $\alpha$ 2B-AR based on the X-ray structure of the h $\beta$ 2-AR, solved at 2.4 Å resolution. The C- and N-terminal parts were not modeled. The final model was stereochemically validated using the PROCHECK<sup>28</sup> program. When necessary, some required refinements of the model were performed with the HyperChem7.52 software.<sup>29</sup> Ligand docking was carried out using the innovative method *Induced Fit* developed by Schrodinger Inc. This method predicts fast and accurate the conformational changes induced by ligand binding to the receptor active sites by merging the docking and scoring capabilities of Glide 4.5<sup>30</sup> with the protein modeling software, Prime 1.6.<sup>31</sup> Both, ligand and receptor have all hydrogen atoms included and the ionization states were set according to the physiological conditions.

## RESULTS and DISCUSSION

### Sequence Alignment

The sequence alignment supplied by the T-coffee server<sup>25,26</sup> was manually refined according to the three dimensional structure of the template, in order to preserve the specific motifs which are highly-conserved in GPCR class and to avoid the gaps in transmembranes. The seven transmembranes have been identified based on the conserved residues within the GPCR amino acid sequences: Gly1.49, Asn1.50 and Val1.53 on the TM1, Ser2.45, Leu2.46, Ala2.47, Ala2.49 and Asp2.50 on TM2, Ser3.40, Leu3.44, Ile3.47, Ser3.48 (Ala3.48 for 2RH1), Asp3.49, Arg3.50, Tyr3.51, Val3.54 on TM3, Trp4.50, Ser4.53 and Pro4.60 on TM4, Phe5.47, Pro5.50, Ile5.53, Tyr5.58 and Ile5.61 (Val5.61 for 2RH1) on TM5, Arg6.32 (Lys6.32 for 2RH1) Phe6.44, Cys6.47, Trp6.48, Pro6.50 on TM6, and Asn7.45, Ser7.46, Asn7.49, Pro7.50, Tyr7.53, Phe7.60 and Arg7.61 on TM7. The amino acids were numbered according to the Ballesteros-Weinstein convention.<sup>32</sup> To facilitate the growth of diffraction-quality crystals of h $\beta$ 2AR, the structure was engineered by replacing the third intracellular loop (IL3) with T4 lysozyme (T4L).<sup>21</sup> This fragment can not be used in the model generation process and we decided not to model the corresponding sequence from  $2\sqrt{B}$  AR between Arg204 and Ala361. The missing parts of the  $2\sqrt{B}$  AR model have no influence on the binding site located in the transmembranar region. The complete alignment before the deletion of the amino acids from the third intracellular loop is shown in Table 1.

### Homology modeling

The model building was carried out with Modeller9v6,<sup>27</sup> which implements an automated approach to comparative protein structure modeling by satisfaction of spatial restraints empirically obtained from a database of protein structure alignments. First, the distance and dihedral angle restraints on the target sequence are calculated from its alignment with template 3D structures. The form of these restraints is obtained from a statistical analysis of the relationships between many pairs of homologous structures. In the next step, the spatial restraints and CHARMM energy terms enforcing proper stereochemistry are combined into an objective function. Finally, the model is refined by optimizing the objective

function in the Cartesian space. The optimization is carried out by using the variable target function

method employing methods of conjugate gradients and molecular dynamics with simulated annealing.

Table 1

Sequence alignment of hα2B-AR (SwissProt ID: ADA2B\_HUMAN, P18089) and β2-AR (PDB code: 2rh1)

2rh1	D	E	V	W	V	V	G	M	G	I	V	M	S	L	I	V	L	A	I	V	F	<b>G</b>	<b>N</b>	V	L	
hα2B	S	V	Q	A	T	A	A	I	A	A	A	I	T	F	L	I	L	F	T	I	F	<b>G</b>	<b>N</b>	A	L	
				.	.	.	:	.	.	.	:	:	:	:	:	*		:	*	*	*	.	*			
2rh1	<b>V</b>	I	T	A	I	A	K	F	E	R	L	Q	T	V	T	N	Y	F	I	T	<b>S</b>	<b>L</b>	<b>A</b>	<b>C</b>	<b>A</b>	
hα2B	<b>V</b>	I	L	A	V	L	T	S	R	S	L	R	A	P	Q	N	L	F	L	V	<b>S</b>	<b>L</b>	<b>A</b>	<b>A</b>	<b>A</b>	
	*	*		*	:	.	.	.	.	*	:	:		*	*	:	.	*	*	*	*	*	*	*	*	
2rh1	<b>D</b>	L	V	M	G	L	A	V	V	P	F	G	A	<b>A</b>	H	I	L	M	K	M	W	T	F	G	N	
hα2B	<b>D</b>	I	L	V	A	T	L	I	I	P	F	S	L	<b>A</b>	N	E	L	L	G	Y	W	Y	F	R	R	
	*	:	:	:	.	.	:	:	*	*	.	*	:	*	:	*	:	*	.	*	.	*	.	.	.	
2rh1	F	W	C	E	F	W	T	S	I	<b>D</b>	V	L	C	V	T	A	<b>S</b>	I	E	T	<b>L</b>	C	V	<b>I</b>	<b>A</b>	
hα2B	T	W	C	E	V	Y	L	A	L	<b>D</b>	V	L	F	C	T	S	<b>S</b>	I	V	H	<b>L</b>	C	A	<b>I</b>	<b>S</b>	
		*	*	*	.	:	:	:	*	*	*	.	*	:	*	*	*	.	*	*	.	*	*	.	*	:
2rh1	V	<b>D</b>	<b>R</b>	<b>Y</b>	F	A	<b>I</b>	T	S	P	F	K	Y	Q	S	L	L	T	K	N	K	A	R	V	I	
hα2B	L	<b>D</b>	<b>R</b>	<b>Y</b>	W	A	<b>V</b>	S	R	A	L	E	Y	N	S	K	R	T	P	R	R	I	K	C	I	
	:	*	*	*	:	*	:	:	.	.	:	*	:	*	:	*	.	*	.	:	.	:	.	.	*	
2rh1	I	L	M	V	<b>W</b>	I	V	<b>S</b>	G	L	T	S	F	L	<b>P</b>	I	Q	M	H	W	Y	R	A	T	H	
hα2B	I	L	T	V	<b>W</b>	L	I	<b>A</b>	A	V	I	S	L	P	<b>P</b>	L	I	Y	K	G	D	Q	G	-	-	
	*	*		*	*	:	:	:	.	:	*	:	*	:	*	:	:	.	.	.	.	:	.	.	.	
2rh1	Q	E	A	I	N	C	Y	A	E	E	T	C	C	D	F	F	T	N	Q	A	Y	A	I	A	S	
hα2B	-	-	-	-	P	Q	P	R	G	R	P	Q	C	K	L	N	Q	E	A	W	Y	I	L	A	<b>S</b>	
					.	.	.	.	.	.	.	*	:	.	.	.	*	.	.	*	.	:	*	*	*	
2rh1	S	I	V	S	<b>F</b>	Y	V	<b>P</b>	L	V	<b>I</b>	M	V	F	V	<b>Y</b>	S	R	V	F	Q	E	A	K	R	
hα2B	S	I	G	<b>S</b>	<b>F</b>	F	A	<b>P</b>	C	L	<b>I</b>	M	I	L	V	<b>Y</b>	L	R	I	Y	L	I	A	K	R	
	*	*		*	*	:	.	*	.	:	*	*	:	:	*	*	.	*	:	:	.	.	*	*	*	
2rh1	Q	L	K	#	#	#	#	#	#	#	#	#	#	#	#	#	#	#	#	#	#	#	#	#	#	
hα2B	S	N	R	R	G	P	R	A	K	G	G	P	G	Q	G	E	S	K	Q	P	R	P	D	H	G	
	.	.	.	:	.	.	.	.	.	.	.	.	.	.	.	.	.	.	.	.	.	.	.	.	.	
2rh1	#	#	#	#	#	#	#	#	#	#	#	#	#	#	#	#	#	#	#	#	#	#	#	#	#	
hα2B	G	A	L	A	S	A	K	L	P	A	L	A	S	V	A	S	A	R	E	V	N	G	H	S	K	
2rh1	#	#	#	#	#	#	#	#	#	#	#	#	#	#	#	#	#	#	#	#	#	#	#	#	#	
hα2B	S	T	G	E	K	E	E	G	E	T	P	E	D	T	G	T	R	A	L	P	P	S	W	A	A	
2rh1	#	#	#	#	#	#	#	#	#	#	#	#	#	#	#	#	#	#	#	#	#	#	#	#	#	
hα2B	L	P	N	S	G	Q	G	Q	K	E	G	V	C	G	A	S	P	E	D	E	A	E	E	E	E	
2rh1	#	#	#	#	#	#	#	#	#	#	#	#	#	#	#	#	#	#	#	#	#	#	#	#	#	
hα2B	E	E	E	E	E	E	E	E	C	E	P	Q	A	V	P	V	S	P	A	S	A	C	S	P	P	
2rh1	#	#	#	#	#	#	#	#	#	#	#	#	#	#	#	#	#	#	#	#	#	#	#	#	#	
hα2B	L	Q	Q	P	Q	G	S	R	V	L	A	T	L	R	G	Q	V	L	L	G	R	G	V	G	A	
2rh1	#	#	#	#	#	#	#	#	#	#	F	C	L	K	E	H	<b>K</b>	A	L	K	T	L	G	I	I	
hα2B	I	G	G	Q	W	W	R	R	R	A	Q	L	T	R	E	K	<b>R</b>	F	T	F	V	L	A	V	V	
	.	.	.	.	.	.	.	.	.	.	.	.	.	*	*	.	.	.	.	.	.	*	.	:	:	
2rh1	M	G	T	<b>F</b>	T	L	<b>C</b>	<b>W</b>	L	<b>P</b>	F	F	I	V	N	I	V	H	V	-	-	I	Q	D	N	
hα2B	I	G	V	<b>F</b>	V	L	<b>C</b>	<b>W</b>	F	<b>P</b>	F	F	F	S	Y	S	L	G	A	I	C	P	K	H	C	
	:	*	.	*	.	*	*	*	:	*	*	*	:	.	.	.	:	.	.	.	.	.	:	.	:	

2rh1	L	I	R	K	E	V	Y	I	L	L	N	W	I	G	Y	V	N	S	G	F	N	P	L	I	Y
hα2B	K	V	P	H	G	L	F	Q	F	F	F	W	I	G	Y	C	N	S	S	L	N	P	V	I	Y
	:				:	:		:	:		*	*	*	*		*	*	*	:	*	*	:	*	*	*
2rh1	C	R	S	P	-	D	<b>F</b>	<b>R</b>	I	A	F	Q	E	L	L	C	L	R	R	S	S	L	K	A	Y
hα2B	T	I	F	N	Q	D	<b>F</b>	<b>R</b>	R	A	F	R	R	I	L	C	R	P	W	T	Q	T	A	W	-
						*	*	*		*	*	:	.	:	*	*				:	.				
2rh1	G	N	G	Y	S	S	N	G	N	T	G	E	Q	S	G										
hα2B	-	-	-	-	-	-	-	-	-	-	-	-	-	-	-										

The amino acid one letter notation is used; “\*” - identical amino acids in both sequences; “:” - amino acids highly similar; “.” - amino acids with low similarity; blank - dissimilar amino acids; bold and italic amino acids - highly conserved amino acids in the GPCR family; shaded amino acids - key amino acids in the ligand binding domain of α2B-AR; “#” - T4L lysozyme fragment in the 2rh1 structure.

The stereochemical validation of the model was performed using the PROCHECK software<sup>28</sup> which verifies the normality of torsion angles, bond angles, bond lengths and distances between unbounded neighbor atoms. The refined 3D model contains 279 residues which are distributed on the Ramachandran map as follow: 258 (92.5 %) are found in the most favored regions (A, B, L regions

or black areas in figure 1), 21 (7.5%) in the additional allowed regions (a, b, l, p regions or dark gray areas in figure 1) and none (0%) in generously allowed (~a, ~b, ~p, ~l regions in figure 1) and disallowed regions (white area in figure 1). The Ramachandran map for the refined 3D model of the α2B-AR based on 2RH1 template is displayed in figure 1.

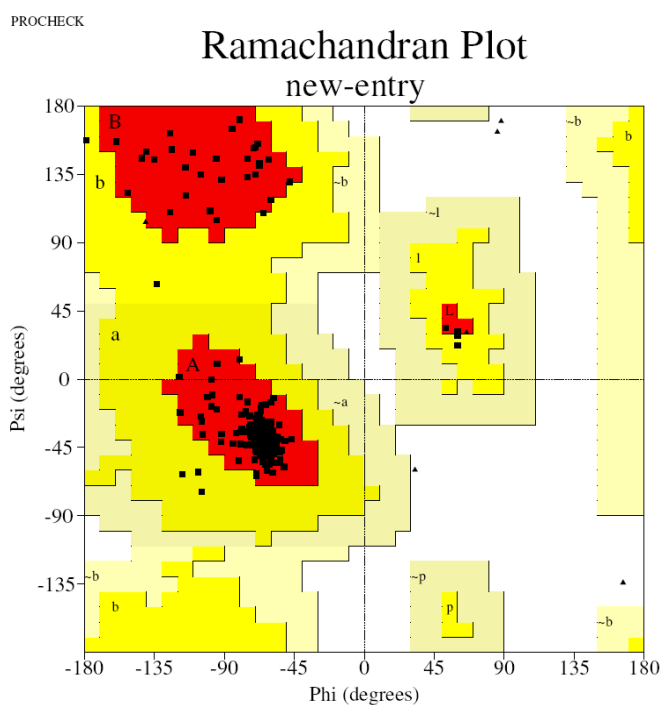


Fig. 1 – Ramachandran map for the homology model of hα2B-AR.

The main-chain parameters (peptide bond planarity, bad non-bonded interactions, Cα distortion, overall G-factor), main-chain bond length distributions, main-chain bond angle distributions, side-chain parameters, were also verified with Procheck. All are in the admitted error limits or better. The 3D model, depicted as solid ribbons is displayed in figure 2.

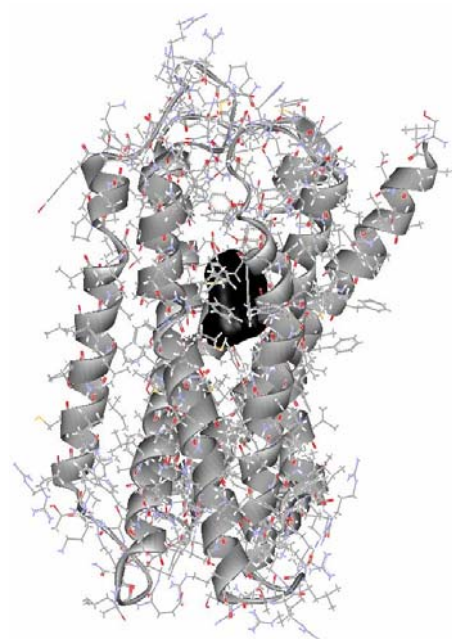


Fig. 2 – The 3D-structure of α2b-AR obtained by homology modeling based on the 2RH1 template; ligand binding pocket is highlighted with dark gray surface.

### Ligand Docking

The ligand binding pocket for the biogenic amine receptors of the GPCR family 1 is located between the TM3, TM5, TM6 and TM7 and functional, spectroscopic and structural data suggest that agonist activation of the amine receptor members of GPCR family 1 is caused by

the movement of these TMs with respect to each other. Using a site-directed mutagenesis experiment,<sup>33</sup> Asp3.32 (Asp92) Ser5.42 (Ser178) and Ser5.46 (Ser180) have been identified as being the key residues involved in ligand binding.

In order to validate the 3D model of  $\alpha$ 2b-AR we used the Schrodinger's Induced Fit (IFD) protocol which combines the scoring capabilities of Glide<sup>30</sup> and the predictive power of Prime<sup>31</sup> to dock norepinephrine, the endogen ligand of all adrenergic receptors. The grid was set to include

the entire protein. Generally, the most common binding mode is given by: (i) an electrostatic interaction between the protonated  $\text{NH}_3^+$  group of the ligand and the deprotonated carboxylate group of Asp92(3.32); (ii) a hydrogen-bond between the 3-OH group of norepinephrine and the OH group of Ser176(5.42) or Ser180 (5.46); (iii)  $\pi$ - $\pi$  interactions between aromatic amino acids and aromatic ring from the ligand.

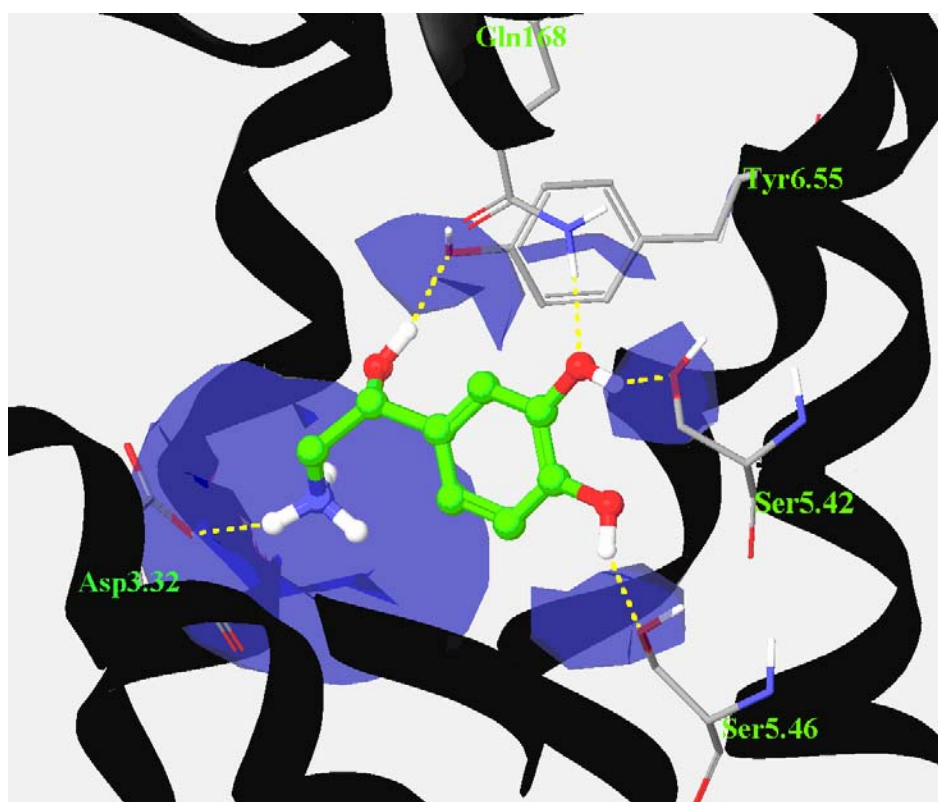


Fig. 3 – The view of norepinephrine into the  $\alpha$ 2B-AR binding site. Norepinephrine is depicted with balls and stick, the receptor with solid ribbons and the residues important for ligand binding with sticks. The hydrophilic regions induced by the ligand are represented with transparent surfaces surrounding the norepinephrine. Dashed lines represent the interactions between ligand and receptor.

The best pose of norepinephrine obtained from docking has the amino and hydroxyl groups pointing toward the TM3 and TM5, respectively. The protonated  $\text{NH}_3^+$  group is favorably placed in the closed vicinity of Asp3.32 and interacts with its negatively charged side-chain, while the 3- and 4-OH groups from catechol ring establish two hydrogen bonds with Ser5.42 and Ser5.46 side-chains. Another two hydrogen bonds between norepinephrine and Tyr391(6.55) and Gln168 from extracellular loop help to stabilize the ligand into the binding site (Figure 3). Another conformation

of norepinephrine which has a docking score close to the best pose presents one hydrogen bond between *meta*-hydroxyl group of norepinephrine and the carboxylate group of Asp92 (3.32) and another one between the  $\beta$ -OH group of norepinephrine and  $\text{NH}_3^+$  group of Asn262. Also, between the catecholic ring and the Trp228(6.48) side-chain a small hydrophobic field can be observed. Both, geometry checking and endogen ligand docking validate the refined 3D model of the human  $\alpha$ 2B-AR obtained based on the X-ray structure of human  $\beta$ 2-AR.

## CONCLUSIONS

Three dimensional model for  $\alpha 2B$ -AR based on X-ray structure of the  $\beta 2$ -AR receptor was built using homology modeling procedure. The model has all the sterical and topological parameters in the normal range. The docking experiment has proven that the final model supports the experimental data obtained through site-directed mutagenesis and provides evidence that it can be used in further studies. The three-dimensional model of the  $\alpha 2B$ -AR will help us to have a better understanding about ligand behavior into the binding site being an important tool for molecular dynamics, pharmacophore and rational drug design studies.

*Acknowledgments:* We thank for financial support to National Council for Scientific Research in Higher Education (CNCSIS), Grant PN-II-PCE-ID nr 1268/Agreement 248/2007; additional agreement 2/2009.

## REFERENCES

1. C. Saunders and L.E. Limbird, *Pharmacol. Ther.* **1999**, *84*,193-205.
2. T.J. Shi, U. Winzer-Serhan, F. Leslie v T. Hokfelt, *Neuroreport*, **1999**, *10*, 2835-2839.
3. J.W. Lomasney, W. Lorenz, L.F. Allen, K. King, J.W. Regan, T.L. Yang-Feng, M.G. Caron and R.J. Lefkowitz, *Proc. Natl. Acad. Sci. U.S.A.*, **1990**, *87*, 5094-5098.
4. R.L. Weinshank, J.M. Zgombick, M. Macchi, N. Adham, H. Lichtblau, T.A. Branchek and P.R. Hartig, *Mol. Pharmacol.*, **1990**, *38*, 681-688.
5. K.P. Makaritsis, D.E. Handy, C. Johns, B.K. Kobilka, I. Gavras and H. Gavras, *Hypertension*, **1999**, *33*, 14-17.
6. R.E. Link, K. Desai, L. Hein, M.E. Stevens, A. D. Bernstein, G.S. Barsh and B.K. Kobilka, *Science*, **1996**, *273*, 803-805.
7. J.W. Kable, L.C. Murrin and D.B. Bylund, *J. Pharmacol. Exp. Ther.*, **2000**, *293*, 1-7.
8. K. Gyires, Z.S. Zádori, N. Shujaa, R. Minorics, G. Falkay and P. Mátyus, *Neurochem Int.*, **2007**, *51*, 289-296.
9. B.A. Graham, D.L. Hammond and H.K. Proudfit, *J. Pharmacol. Exp. Ther.*, **1997**, *283*, 511-519.
10. S. Sawamura, W.S. Kingery, M.F. Davies, G.S. Agashe, J.D. Clark, B.K. Kobilka, T. Hashimoto and M. Maze, *J. Neurosci*, **2000**, *20*, 9242-9251.
11. R. Gáspár, A. Gál, M. Gálik, E. Ducza, R. Minorics, Z. Kolarovszki-Sipiczki, A. Klukovits and G. Falkay, *Neurochem. Int.*, **2007**, *51*, 311-318.
12. L. Hein, L.E. Limbird, R.M. Eglén and B.K. Kobilka, *Ann. N.Y. Acad. Sci.*, **1999**, *881*, 265-271.
13. V. Muthig, R. Gilsbach, M. Haubold, T. M. Gessler and L. Hein, *Circ. Res.*, **2007**, *101*, 682-691.
14. K.M. Small, K.M. Brown, S.L. Forbes and S.B. Liggett, *J. Biol. Chem.*, **2001**, *276*, 4917-4922.
15. C. Cayla, P. Heinonen, L. Viikari, S. Schaak, A. Snapir, A. Bouloumie, M.K. Karvonen, U. Pesonen, M. Scheinin and H. Paris, *Biochem. Pharmacol.*, **2004**, *67*, 469-478.
16. R. Vasudevan, P. Ismail, J. Stanslas, N. Shamsudin and A.B. Ali, *Int. J. Biol. Sci.*, **2008**, *4*, 362-367.
17. N. Papanas, K. Papatheodorou, D. Papazoglou, S. Kotsiou, D. Christakidis and E. Maltezos, *Exp Clin. Endocrinol. Diabetes*, **2007**, *115*, 327-330.
18. D. Papazoglou, N. Papanas, K. Papatheodorou, S. Kotsiou, D. Christakidis and E. Maltezos, *Exp. Clin. Endocrinol. Diabetes*, **2006**, *114*, 424-427.
19. D.J. de Quervain, I.T. Kolassa, V. Ertl, P.L. Onyut, F. Neuner, T. Elbert and A. Papassotiropoulos, *Nat. Neurosci.*, **2007**, *10*, 1137-1139.
20. B. Ohlin, G. Berglund, P.M. Nilsson and O. Melander, *J. Hypertens.*, **2007**, *25*, 1613-1619.
21. V. Cherezov, D.M. Rosenbaum, M.A. Hanson, S.G. Rasmussen, F.S. Thian, T.S. Kobilka, H.J. Choi, P. Kuhn, W.I. Weis, B.K. Kobilka and R.C. Stevens, *Science*, **2007**, *318*, 1258-1265.
22. H. Xhaard, T. Nyronen, V.-V. Rantanen, J. O. Ruuskanen, J. Laurila, T. Salminen, M. Scheinin and M.S. Johnson, *J. Struct. Biol.*, **2005**, *150*, 126-143.
23. B. Balogh, A. Szilágyi, K. Gyires, D.B. Bylund and P. Mátyus, *Neurochem. Int.*, **2009**, *55*, 355-361.
24. UniProtKB/Swiss-Prot, <http://www.expasy.org/sprot/sprot-top.html>, accessed in 2009.
25. C. Notredame, D.G. Higgins and J. Heringa, *J. Mol. Biol.*, **2000**, *302*, 205-217.
26. (a) O. Poirot, E. O'Toole and C. Notredame, *Nucleic Acids Res.* **2003**, *31*, 3503-3506;  
(b) Sali and T.L. Blundell, *J. Mol. Biol.* **1993** *234*, 779-815.
27. L.A. Laskowski, M.W. MacArthur, D.S. Moss and J.M. Thornton, *J. Appl. Cryst.*, **1993**, *26*, 283-291.
28. HyperChem 7.52 release for Windows; HyperCube, Inc., **2006**.
29. Glide 4.5; Schrodinger, LLC, 2008.
30. Prime 1.6; Schrodinger, LLC, 2008.
31. J.A. Ballesteros, L. Shi and J.A. Javitch, *Mol. Pharmacol.*, **2001**, *60*, 1-19.
32. C.-D. Wang, M.A. Buck and C.M. Fraser, *Mol. Pharmacol.*, **1991**, *40*, 168-179.